JOURNAL OF GEOPHYSICAL RESEARCH, VOL. 106, NO. B6, PAGES 11,017–11,030, JUNE 10, 2001

Superplastic deformation of ice: Experimental observations

D. L. Goldsby[1] and D. L. Kohlstedt

Department of Geology and Geophysics, University of Minnesota-Twin Cities
Minneapolis, Minnesota

Abstract. Creep experiments on fine-grained ice reveal the existence of three creep regimes: (1) a dislocation creep regime, (2) a superplastic flow regime in which grain boundary sliding is an important deformation process, and (3) a basal slip creep regime in which the strain rate is limited by basal slip. Dislocation creep in ice is likely climb-limited, is characterized by a stress exponent of 4.0, and is independent of grain size. Superplastic flow is characterized by a stress exponent of 1.8 and depends inversely on grain size to the 1.4 power. Basal slip limited creep is characterized by a stress exponent of 2.4 and is independent of grain size. A fourth creep mechanism, diffusional flow, which usually occurs at very low stresses, is inaccessible at practical laboratory strain rates even for our finest grain sizes of ~3 μm. A constitutive equation based on these experimental results that includes flow laws for these four creep mechanisms is described. This equation is in excellent agreement with published laboratory creep data for coarse-grained samples at high temperatures. Superplastic flow of ice is the rate-limiting creep mechanism over a wide range of temperatures and grain sizes at stresses $\lesssim$ 0.1 MPa, conditions which overlap those occurring in glaciers, ice sheets, and icy planetary interiors.

1. Introduction

The dynamical properties of glaciers and ice sheets are controlled in large part by the grain-scale deformation of ice. To better understand the rheological behavior of ice and to develop a constitutive equation that can be used to model the flow behavior of natural ice bodies, we carried out laboratory deformation experiments on ice I [*Goldsby et al.,* 1993; *Goldsby and Kohlstedt,* 1995a, 1995b, 1997a, 1997b, 1997c]. A key feature of our investigation was the use of fine-grained samples that allowed us to explore deformation not only by grain matrix dislocation processes but also by grain size sensitive flow mechanisms involving grain boundary sliding (GBS) and diffusion.

One of the exciting discoveries in our study is that ice exhibits an extensive creep regime in which GBS contributes substantially to flow, a regime often described as superplastic deformation. Superplasticity is classically defined phenomenologically as the ability of a material to be deformed in tension to large strains, typically >>100% [e.g., *Davies et al.,* 1970; *Ridley*, 1995]. Although our experiments were carried out in compression rather than tension, we have adopted the term superplastic to characterize our results because the mechanism of deformation appears to be the same as that described in the materials science literature and because the stress exponent in equation (1) is $\lesssim$2, as observed for superplastic flow. In the present paper, we detail the results of our recent laboratory experiments on the rheology of ice in order to develop a constitutive equation which we compare with results of other laboratory experiments on ice. In a paper in preparation (D.L. Goldsby and D.L. Kohlstedt, manuscript in preparation, 2001), we will explore the implications of this superplastic creep regime for the flow of natural ice bodies by comparing our constitutive equation with field observations on glaciers and ice sheets. In a recent paper our results were used in state-of-the-art thermomechanical models of the modern Greenland ice sheet and the ancient Laurentide ice sheet to simultaneously explain the forms of these cryospheric structures [*Peltier et al.*, 2000], a situation not possible with the flow law commonly used to describe the rheological behavior of ice.

2. Background

Rheological data for crystalline materials are typically analyzed with a power law relationship of the form

$$\dot{\varepsilon} = A \frac{\sigma^n}{d^p} \exp\left(-\frac{Q + PV}{RT} \right), \quad (1)$$

where $\dot{\varepsilon}$ is strain rate, A is a material parameter, σ is differential stress, n is the stress exponent, d is grain size, p is the grain size exponent, Q is the activation energy for creep, P is the hydrostatic pressure, V is the activation volume for creep, R is the gas constant, and T is absolute temperature. Tables 1-4 summarize published values of the creep parameters for both single-crystal and polycrystalline ice in the form expressed in (1).

Table 1 emphasizes dislocation creep parameters for single crystals oriented for easy (basal) slip. Most experiments yield a stress exponent of 2 to 2.5. Measured values of activation energy typically vary between 60 and 80 kJ mol^{-1} at temperatures $\gtrsim$ 250 K, with most closer to 60 kJ mol^{-1}. *Jones and Glen* [1968] noted a marked decrease to a value of 40 kJ mol^{-1}

[1]Now at Department of Geological Sciences, Brown University, Providence, Rhode Island.

Paper number 2000JB900336.
0148-0227/01/2000JB900336$09.00

Table 1. Creep Parameters n and Q for Ice Single Crystals Oriented for Basal Slip

Reference	n	Q, kJ mol^{-1}	Comments
Steinemann [1954]	1.5 - 3.9		constant σ
Griggs and Coles [1954]	~2		constant σ
Butkovitch and Landauer [1958]	2.5		constant σ
Readey and Kingery [1964]	2 - 2.5	59.8	constant $\dot{\varepsilon}$
Wakahama [1967]	2.3		constant $\dot{\varepsilon}$
Jones and Glen [1968]	~2.3	40 ± 2	constant σ, 203 < T < 223 K
Jones and Glen [1968]		68	constant $\dot{\varepsilon}$, 203 < T < 253 K
Jones and Glen [1969]	2 - 3	42 - 75	constant $\dot{\varepsilon}$
Jones and Glen [1969]	~2.3	65 ± 3	constant σ
Ramseier [1972]	2.5	59.5	constant σ
Ramseier [1972]	~2		constant $\dot{\varepsilon}$
Homer and Glen [1978]	~2	78 ± 4	constant σ

in constant stress experiments at lower temperatures in the range 203-223 K. However, from the results of their constant strain rate tests we calculated an activation energy of 68 kJ mol^{-1} in the same temperature range. The constant strain rate tests were conducted to much larger strains than the constant stress tests, suggesting that the lower value for activation energy from the latter may reflect contributions from transient creep to the strain rate at small strains.

The rheology of ice single crystals oriented for hard (nonbasal) slip has also been investigated [e.g., *Nakaya*, 1958; *Butkovitch and Landauer*, 1958; *Higashi*, 1967; *Wakahama*, 1967; *Mellor and Testa*, 1969a] (I. Andermann, unpublished work as cited by *Duval et al.*[1983]). Slip is more difficult on prismatic planes than on the basal plane and is even more difficult on pyramidal slip systems [*Duval et al.*, 1983]. At a given stress and temperature, single crystals oriented for basal slip can strain >10^5 times faster than crystals oriented for nonbasal slip. Experiments on single crystals oriented for hard slip are therefore extremely difficult to conduct accurately because slight sample misorientation results in a significant contribution from basal slip. While strength data exist for hard slip, the creep parameters n and Q have not been reliably determined.

Table 2 summarizes creep parameters for polycrystalline aggregates deformed at ambient pressure. Nearly all of these experiments were performed on samples with large grains, ≥1 mm. Most of the experiments listed in Table 2 yielded stress exponents of ~3, though experiments that explore stresses above ~1 MPa produced stress exponents of ~4 [e.g., *Steinemann*, 1954, 1958; *Barnes et al.*, 1971]. The value of $n \approx 3$ has generally been taken to be indicative of dislocation creep of ice. Below ~263 K, measured values for activation energy typically range from 60 to 80. Above ~263 K, an apparent increase in the activation energy occurs in the $n \approx 3$ region. This increase in Q, which is not observed for ice single crystals [*Homer and Glen*, 1978], has been associated with premelting at grain boundaries [e.g., *Dash et al.*, 1995].

Table 3 summarizes the creep parameters from a large body of experiments carried out in the dislocation creep field for ice samples with grain sizes ≥200 μm deformed at high confining pressures [*Kirby et al.*, 1987; *Durham et al.*, 1988, 1992, 1997]. These experiments consistently yield a stress exponent of 4.0 over a large range of temperature and stress. Between 195 and 240 K, the activation energy is 61 kJ mol^{-1}; the apparent activation energy increases to 91 kJ mol^{-1} for the temperature range 240-258 K.

Finally, Table 4 summarizes creep data from a number of studies on coarse-grained (d ≥1 mm) polycrystalline ice in which the stress exponent decreases to <2 at stresses ≤0.2 MPa. This decrease in the stress exponent has been

Table 2. Creep Data for Polycrystalline Ice

Reference	n	Q_{creep}, kJ mol^{-1}	Comments[a]
	T ≤ 263 K		
Glen [1955]	~3		
Steinemann [1958]	3.1-3.6	83	
Mellor and Smith [1966]	3.5	45	
Mellor and Testa [1969a]		67.5	
Barnes et al. [1971]	3.1	77	
Ramseier [1972]	2.5	59.9	columnar ice
Ramseier [1972]	3.1	59.9	
Gold [1973]		65	columnar ice
Hawkes and Mellor [1972]	3		
	T > 263 K		
Glen [1955]	3.2	135	
Steinemann [1958]	2.8-3.2	135	
Mellor and Testa [1969a]	3.2	167	
Barnes et al. [1971]	3.2	120	

[a]Reported grain sizes for listed studies are ≥1 mm.

Table 3. Flow Law Parameters for Ice I at $P_c = 50$ MPa

T, K	$\log_{10} A$, $MPa^{-n} s^{-1}$	n	Q, kJ mol^{-1}	V, m^3 mol^{-1}	Reference
240-258	11.8±0.4	4.0±0.6	91±2	-13×10^{-6} [a]	*Kirby et al.* [1987]
195-240	5.10±0.03	4.0±0.1	61±2	$-13\pm3\times10^{-6}$	*Kirby et al.* [1987]
140-195	-2.8±0.6	6.0±0.4	39±5	-13×10^{-6} [a]	*Durham et al.* [1997]

[a]Values are estimated, not measured [*Durham et al.*, 1997].

attributed to the influence of a different creep mechanism such as diffusional flow at low stresses [e.g., *Mellor and Smith*, 1966].

To provide a framework for further discussion, stress-strain rate data from a number of experiments listed in Tables 1-4 are compared in Figure 1. Data are normalized to a common temperature using reported activation energies if available or values of 78 kJ mol^{-1} below 265 K and 120 kJ mol^{-1} above 265 K as given by *Frost and Ashby* [1982]. In addition, a subset of the data from hard slip of single crystals is included. Nearly all of the data for polycrystalline samples in Figure 1 are for grains ≥1 mm in size.

As demonstrated in Figure 1, the flow of polycrystalline ice is characterized by a stress exponent of 4.0 at the highest stresses, on the basis of results obtained at high pressures at stresses of 1 to 100 MPa [e.g., *Durham et al.,* 1992] and at ambient pressure at stresses of 1 to 10 MPa [e.g., *Steinemann*, 1954; *Barnes et al.*, 1971]. The creep strength of polycrystalline ice in this $n = 4.0$ regime is intermediate between the strengths of single crystals oriented for easy slip and hard slip, suggesting that creep of polycrystalline ice in this regime requires activation of dislocations on the hard slip systems.

One of the interesting features to note in Figure 1 is that with decreasing stress the log-log plot of $\dot{\varepsilon}$ versus σ for polycrystalline ice is markedly curved. This curvature suggests a change in stress exponent near a stress of 1 MPa and a strain rate of 10^{-8} s^{-1} from $n \approx 4$ at high stresses to $n \approx 2$ at lower stresses. However, because the data acquired at the lower stresses were obtained at extremely slow strain rates ($<10^{-9}$ s^{-1}) and consequently very small strains, they may be indicative of transient rather than steady state dislocation creep [e.g., *Weertman*, 1983]. In this case, the transition with decreasing stress from $n \approx 4$ to $n \approx 2$ is not a reliable indicator of a transition between two steady state creep processes. The extremely slow strain rates ($<10^{-9}$ s^{-1} yields <1% strain in ~100 days) at which these experiments on coarse-grained ice were conducted make it impossible to determine reliable values for the steady state creep parameters necessary to describe the effects of stress, temperature, and grain size on strain rate. Without these parameters the rate-controlling creep mechanism(s) at low stress cannot be identified. Because the strain rate in a grain size sensitive flow regime such as diffusional flow increases with decreasing grain size, the investigation of grain size sensitive creep mechanisms is best pursued on fine-grained samples.

We therefore conducted a study of the rheology of fine-grained ice to identify the rate-controlling, steady state creep mechanisms that likely operate at the low stresses important for the flow of glaciers, ice sheets, and icy planetary bodies [*Goldsby and Kohlstedt*, 1997a]. Using these fine-grained samples, we have unambiguously identified a grain size sensitive creep mechanism for ice at practical laboratory strain rates. In the following sections, we first briefly summarize creep results from *Goldsby and Kohlstedt* [1997a]. We then present new experimental data in order to formulate a constitutive equation which includes our newly discovered creep mechanisms for ice.

3. Experimental Methods

Two points were critical in our creep experiments. First, recently developed sample fabrication techniques made it possible to systematically vary the grain size in our samples from 3 to 200 μm. Second, compressive creep experiments were conducted in a high resolution 1 atm deformation apparatus [*Mackwell et al.*, 1990] modified for cryogenic use. These two refinements enabled us to investigate the rheology

Table 4. Low Stress Creep Data for Coarse-Grained Ice [a]

Reference	d, mm	n	p	T, K	Q, kJ mol^{-1}
Steinemann [1954]	0.5-5	1.85		268	
Glen [1955]		~1.5		260-273	
Jellinek and Brill [1956]	1-2	~1		258-268	67
Butkovitch and Landauer [1960]	3-20	0.86-1.15		254-272	60
Mellor and Smith [1966]	0.8	~1		238-273	75
Bromer and Kingery [1968]	1-10	~1	1.95	260-270	50
Mellor and Testa [1969b]	1	1.8		271	
Colbeck and Evans [1973][b]	2	1.3		273	
Baker [1978a, 1978b]	0.6-1	2.8, 3.7	2.35[c]	~265	
Pimienta and Duval [1987]	1-2	~1.5		258	
Duval and Castelnau [1995]	1	1.8		260	

[a]All of the table data were acquired over a stress range of 0.01 to 1 MPa.
[b]Compression experiments were performed inside a glacier tunnel; creep samples were large blocks cut from tunnel.
[c]Below a grain size of 1 mm; p=2.35; grain size dependence is -2.5 at grain sizes >1 mm..

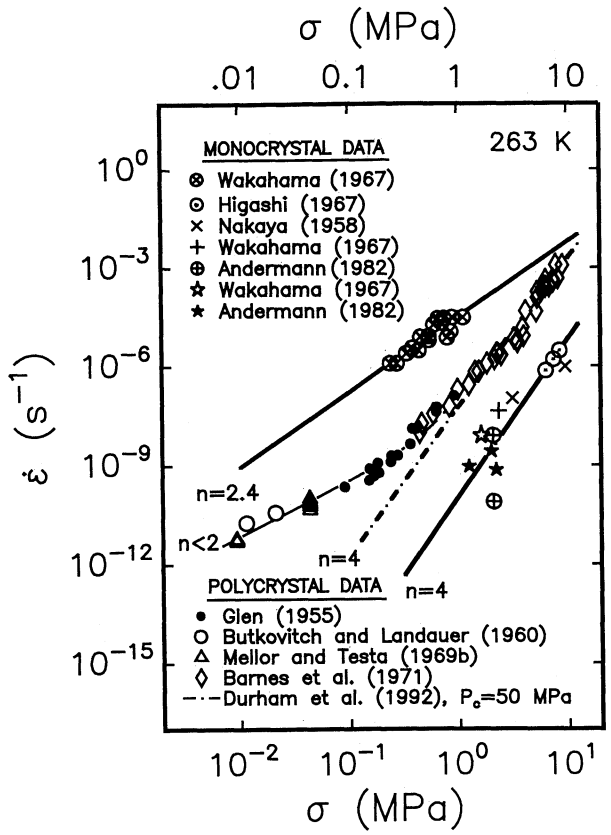

Figure 1. (a) Log-log plot of $\dot{\varepsilon}$ versus σ comparing data for polycrystalline ice and single crystals oriented for basal and nonbasal slip. Data have been normalized (when necessary) to 263 K. Basal slip single crystals are characterized by a stress exponent of ~2.4; nonbasal slip single crystals are characterized by a stress exponent close to 4. At high stresses the stress exponent for polycrystalline samples is 4; at low stresses the data suggest a transition to $n \lesssim 2$. Note that Glen's experimental data lie in the vicinity of the transition between creep regimes characterized by n=4 and $n \lesssim 2$.

of ice at temperatures between 170 and 268 K, differential stresses of 0.2 to 20 MPa, and hence strain rates of 10^{-8} to 10^{-4} s^{-1}. With this wide range of experimental conditions we were able to quantify the flow laws for both dislocation creep and grain size sensitive flow. Often both creep regimes could be explored with a single sample of appropriate grain size.

3.1. Sample Preparation

Samples were fabricated by hot pressing fine-grained ice powders into fully dense aggregates. These fine-grained powders were formed by spraying a mist of distilled water into a reservoir of liquid nitrogen to form an ice/liquid nitrogen slurry. Ice powders with particle sizes < 25 μm were separated from this slurry by sieving. These powders were then packed into the stainless steel cylinder and hot pressed under an axial stress of 100 MPa at a temperature of 196 K for a period of ~2 hours. This technique yielded uniform grain sizes of ~30-40 μm, as determined using a line intercept technique with a correction factor of 1.5. Samples were ~10 mm in diameter and ~20 mm in length.

Finer-grained samples were fabricated using a modified version of the technique of *Durham et al.* [1994]. Samples fabricated as described above were pressurized inside the molding cylinder into the ice II stability field by applying an axial stress of ~300 MPa. After a brief equilibration time the axial stress was quickly decreased to bring the sample back into the ice I field. The pressure was then adjusted to 100 MPa, and the sample was hot pressed for an additional 2 hours. This technique yielded fully dense samples with uniform grain sizes of 3-5 μm.

Finally, samples with grain sizes > 30-40 μm were formed either by annealing 30-40 μm samples at elevated temperatures or by hot pressing coarser-grained powders. Coarser-grained powders with particle sizes between 0 and ~200 μm were formed by grinding laboratory grown ice in a coffee grinder in a cold chamber. These coarser particles were then sieved to obtain particle sizes between 175 and 200 μm. The powders were packed into a stainless steel molding cylinder and hot pressed in the exact manner described for the finer-grained samples.

3.2. Mechanical Testing

Creep experiments were conducted in a high-resolution dead weight load apparatus [*Mackwell et al.*, 1990] fitted with a cold chamber to permit control of sample temperature for $170 \leq T \leq 273$ K. The large thermal mass of the cold cell limited temperature fluctuation to ±0.5 K at ≤233 K and to ±0.25 K at >233 K. The maximum temperature gradient across the sample was 0.05 K mm^{-1}.

Changes in sample length were measured by monitoring the spacing between two machineable glass ceramic plates, one positioned directly above and the other directly below the sample. The body of a linear variable displacement transducer (LVDT) was mounted outside the cold cell on thin machineable glass ceramic sensor rods attached to the top sample plate, while the LVDT core was attached to sensor rods attached to the bottom plate. The use of an identical material for the plates above and below the sample and for the LVDT sensor rods minimizes the effect of thermal expansion or contraction of these load train components on the creep curve. The resolution of this apparatus allow experiments at strain rates as slow as 1×10^{-8} s^{-1}.

3.3. Microstructural Analyses

Deformed samples were analyzed in an environmental scanning electron microscope (ESEM) modified for low-temperature use. Higher pressures can be maintained in the sample chamber of an ESEM than in a conventional SEM, allowing sublimation of ice samples. To reveal grain size and shape, grain boundaries were thermally etched at 200 to 230 K. The cold stage allowed samples to be analyzed at temperatures as low as 170 K.

4. Experimental Data

A subset of our creep data for samples with grain sizes of ~8-200 μm is plotted as log $\dot{\varepsilon}$ versus log σ in Figure 2a. Included in Figure 2a are the flow laws for single crystals oriented for basal slip [*Wakahama*, 1967] and for dislocation creep of polycrystalline ice at high pressure [*Durham et al.*, 1992]. The high-pressure data were normalized from a confining pressure of 50 MPa to atmospheric pressure using an activation volume of ~ 13×10^{-6} m^3 mol^{-1} [*Kirby et al.*, 1987]. (The sample with a grain size of 200 μm was deformed at 268 K and extrapolated to 236 K using the appropriate activation energies, as described below.)

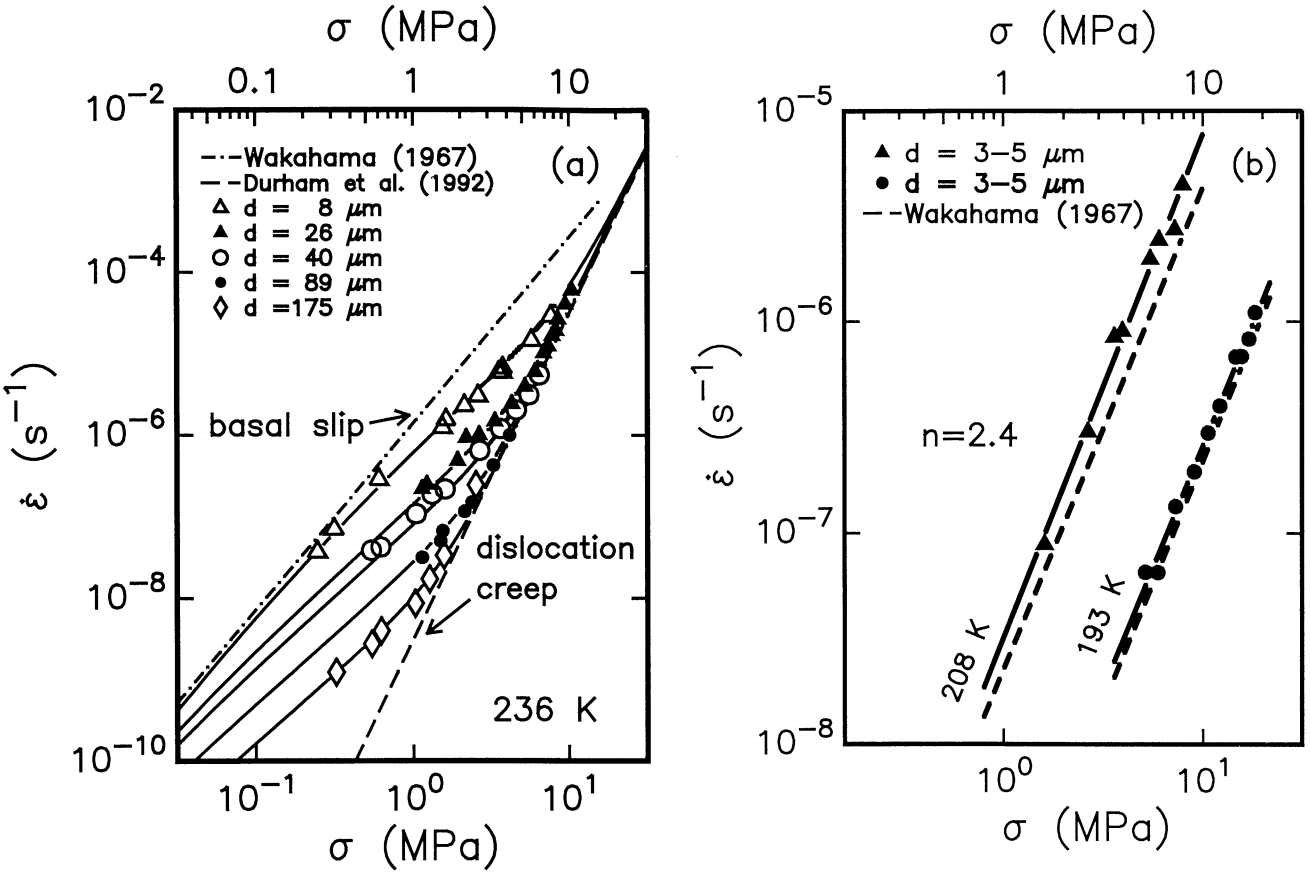

Figure 2. (a) Log-log plot of $\dot{\varepsilon}$ versus σ for fine-grained samples with grain sizes of 8 to 175 μm. All of the samples except the 175-μm sample were deformed at 236 K. Data for the 175-μm sample were extrapolated from 248 K. Three creep regimes can be identified: an n=4 regime at the highest stresses, an n=1.8 regime at intermediate stresses, and an n=2.4 regime at the lowest stresses (for the finest-grained samples). The dislocation creep flow law of *Durham et al.* [1992] and the basal slip single crystal rheology of *Wakahama* [1967] are included for comparison. (b) Log-log plot of $\dot{\varepsilon}$ versus σ showing data for samples with grain sizes of 3-5 μm deformed at 193 and 208 K in the n=2.4 regime.

Three separate creep regimes can be identified in Figure 2a. At the highest stresses, flow of our fine-grained samples is characterized by a stress exponent of 4.0. In this n = 4.0 regime the strain rate is independent of grain size, and the activation energy is 64 kJ mol^{-1} [*Goldsby and Kohlstedt*, 1997a, Figures 3 and 4].

With decreasing stress a transition occurs to a creep regime characterized by n = 1.8. The strain rate in this regime is dependent upon grain size with a grain size exponent p = 1.4 and an activation energy of 49 kJ mol^{-1} [*Goldsby and Kohlstedt*, 1997a, Figures 3 and 4].

At lower stresses, Figure 2a reveals a transition for the finest-grained samples to a creep regime characterized by n = 2.4. Data for samples with grain sizes of 3-5 μm that were deformed at lower temperatures of 193 and 208 K also yield a stress exponent of 2.4, as shown in Figure 2b. The strain rate in this n = 2.4 regime is independent of grain size, and the activation energy is ~60 kJ mol^{-1} [*Goldsby and Kohlstedt*, 1997a, Figure 4].

4.1. Large Strain Experiments

We also conducted two experiments to large compressive strains, one each in the n = 1.8 and n = 2.4 creep regimes; these samples were subjected to total strains of 0.75 and 0.88 at temperatures of 236 and 208 K, respectively [*Goldsby and Kohlstedt*, 1997a]. One of the purposes of these experiments was to generate and observe the microstructures produced at large strains. The creep curve from the experiment in the n = 1.8 regime [*Goldsby and Kohlstedt*, 1997a, Figure 5] indicates a steady state creep rate for strains from 0 to 0.5; at larger strains, the strain rate is a factor of ~1.15 larger. In contrast, significant work hardening (i.e., decrease in strain rate with increase in strain) occurred during the experiment in the n = 2.4 creep regime.

The amount of grain flattening in the sample deformed in the n = 1.8 regime was much less than expected for a macroscopic strain of 0.75 [*Goldsby and Kohlstedt*, 1997a, Figure 6]. In addition, numerous four-grain junctions not present in undeformed samples were observed in this specimen. Finally, the sample was transparent after the experiment; a page of text could be viewed clearly through a 10-mm-thick sample, indicating that the sample was free of cavities and microcracks. In contrast, the grains in the sample deformed in the n = 2.4 regime were flattened significantly, consistent with the overall work hardening (due to dislocation entanglement) observed during the experiment.

4.2. Experiments on Samples With Large Grain Sizes

Since the publication of *Goldsby and Kohlstedt* [1997a], we have conducted two additional experiments on samples with larger grain sizes of 175-200 μm. Creep results for a sample deformed at 248 K are presented in the log-log plot of $\dot{\varepsilon}$ versus σ in Figure 3a. Creep data from a sample with a grain size of 26 μm that was deformed at 236 K (shown in Figure 2a) are also shown in Figure 3a; these data were extrapolated from 236 to 248 K using an activation energy of 49 kJ mol^{-1}. Figure 3a also includes extrapolations not only of the data for the 26-μm sample to a grain size of 175 μm using grain size exponents of p = 1.4 and 3 but also the dislocation creep flow law from the high-pressure experiments of *Durham et al.* [1992]. For the 175-μm sample the stress exponent decreases with decreasing stress from 4.0 to ~1.8 near a stress of 2 MPa.

Another experiment was performed near the melting point. Creep results from this experiment at 268 K are shown in Figure 3b. Again, creep data from a 26-μm sample deformed at 236 K (see Figure 2a) are included for comparison. These data were extrapolated from 236 to 258 K using an activation energy of 49 kJ mol^{-1} and from 258 K to 268 K using an apparent activation energy of 192 kJ mol^{-1}. Also included in Figure 3b are extrapolations of the data for the 26-μm sample to a grain size of 200 μm using grain size exponents of 1.4 and 3 as well as the dislocation creep flow law of *Durham et al.* [1992]. Data for the 200 μm sample yield a transition with decreasing stress from a stress exponent of 4.0 to a stress exponent of ~1.8 near a stress of ~1 MPa.

4.3. Enhanced Creep Rates in the n=1.8 and n=4.0 Creep Regimes Above 258 K

Enhancements in creep rate above ~258 K give rise to an increase in the apparent activation energy in both the n = 1.8 and n = 4.0 creep regimes. The activation energy in the n = 1.8 regime is 49 kJ mol^{-1} below~258 K [*Goldsby and Kohlstedt*, 1997a, Figure 4]. Since our earlier paper, we determined experimentally that the apparent activation energy in the n = 1.8 regime increases from 49 to ~190 kJ mol^{-1} above 258 K, as shown in the Arrhenius plot in Figure 4.

A similar creep rate enhancement occurs in the n = 4.0 regime at temperatures above ~258 K. This enhancement is difficult to quantify, however, because few creep data exist from this regime. The method used to constrain this strain rate enhancement is described below.

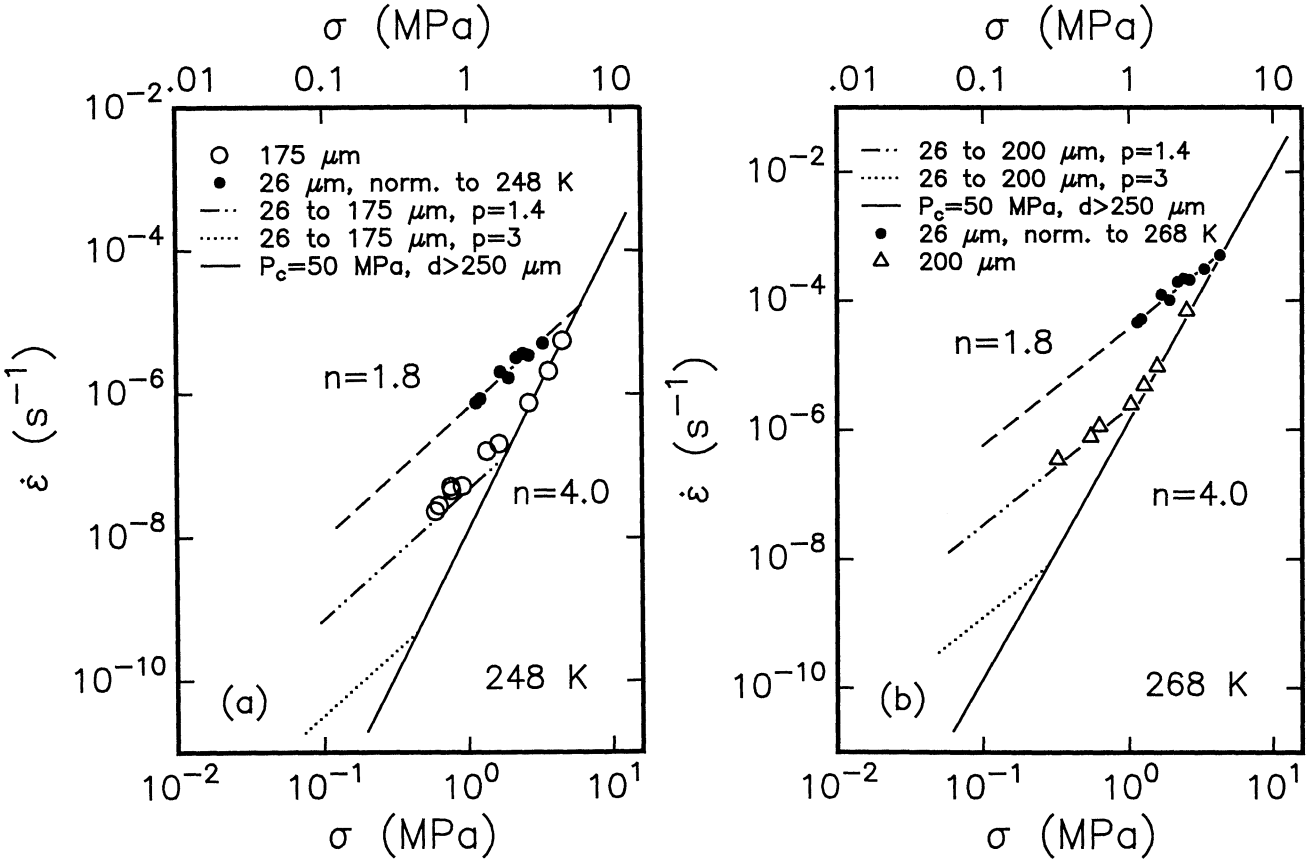

Figure 3. Creep data for larger-grained samples. (a) Data for a 175-μm sample deformed at 248 K are compared with data for the 26-μm sample; the latter were normalized to 248 K using an activation energy of 49 kJ mol^{-1}. Extrapolations of the data for the 26-μm sample to a grain size of 175 μm using grain size exponents of 1.4 and 3 are also shown. (b) Data for a 200-μm sample deformed at 268 K are compared with data for a 26-μm sample; the latter were normalized to 255 K using an activation energy of 49 kJ mol^{-1}, then from 255 to 268 K using an apparent activation energy of 192 kJ mol^{-1}. Extrapolations of the data for the 26-μm sample to a grain size of ~200 μm using grain size exponents of 1.4 and 3 are shown for comparison.

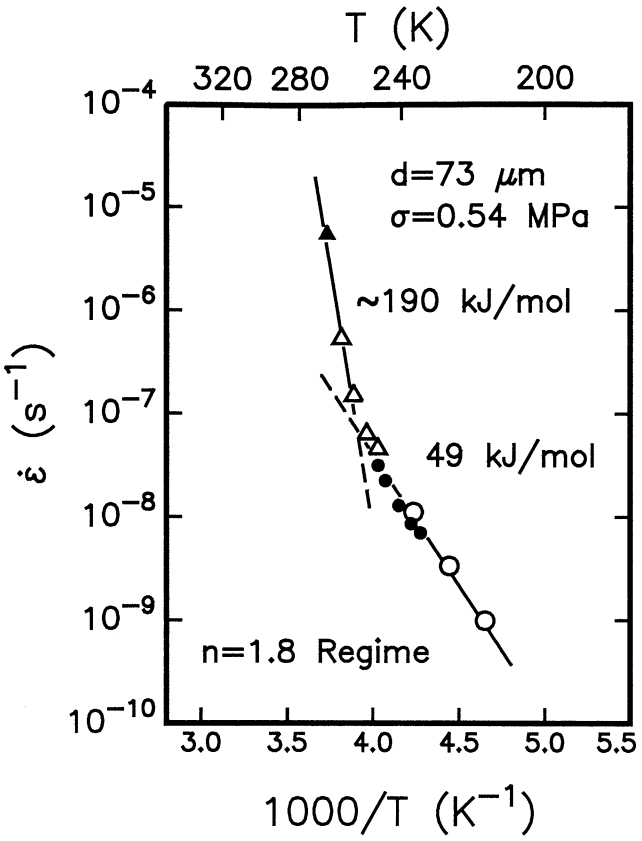

Figure 4. Arrhenius plot illustrating the increase in activation energy in the n=1.8 regime above ~258 K. Creep rates were normalized to a grain size of 73 μm.

5. Discussion

Our experiments reveal the existence of three distinct creep regimes for ice. At the highest stresses the flow of ice is characterized by a stress exponent of 4.0. This value of n is in excellent agreement with the value determined in high confining pressure experiments [*Durham et al.*, 1992] (see Table 4). The activation energy in the $n = 4.0$ creep regime in our experiments, 64 kJ mol^{-1}, and in the high-pressure experiments, 61 kJ mol^{-1}, is in good agreement with values for volume self-diffusion of hydrogen and oxygen in ice, ~60 kJ mol^{-1} [e.g., *Ramseier*, 1967a, 1967b]. The creep rate in this $n = 4.0$ regime is independent of grain size. A value of the stress exponent of 4.0 and the invariance of the strain rate with grain size indicate flow via dislocation creep. In addition, the equivalence of the activation energy for creep with that for self-diffusion suggests that the creep rate in this regime is limited by dislocation climb [e.g., *Weertman*, 1968].

With decreasing stress a transition occurs to a creep regime characterized by a stress exponent of 1.8. The activation energy in this $n = 1.8$ regime is 49 kJ mol^{-1}, a value significantly smaller than in the $n = 4$ regime. The flow of ice in this regime is markedly dependent on grain size with a grain size exponent of 1.4; a portion of these results have recently been duplicated in creep experiments on fine-grained ice samples at high confining pressure [*Durham et al.*, this issue]. One might expect that creep experiments on very fine-grained ice samples might reveal a transition from dislocation creep to diffusional flow at low stresses. However, the stress exponent of 1.8 and grain size exponent of 1.4 do not agree well with values indicative of diffusional flow, that is, $n = 1$ with $p = 2$ for creep controlled by volume diffusion (Nabarro-Herring creep [*Nabarro*, 1948; *Herring*, 1950]) and $n = 1$ with $p = 3$ for creep controlled by grain boundary diffusion (Coble creep [*Coble*, 1963]).

5.1. Superplastic Flow

The creep parameters in the $n = 1.8$ regime are in better agreement with those determined experimentally for flow within region II of the superplastic deformation regime than for flow within the diffusional creep field [e.g., *Ball and Hutchison*, 1969; *Mukherjee*, 1971; *Langdon*, 1970, 1994; *Kaibyshev*, 1992]. Superplastic flow in region II is typically characterized by a flow law of the form $\dot{\varepsilon} \propto \sigma^2/d^2$.

In the $n = 1.8$ regime, not only is the mechanical behavior markedly different, but also the microstructures are strikingly different from those in the dislocation creep regime. No significant grain flattening occurs in the $n = 1.8$ creep regime in axial compression to a strain of ~0.75 [*Goldsby and Kohlstedt*, 1997a, Figures 5 and 6], consistent with deformation in a creep regime in which GBS contributes significantly to the macroscopic strain. Furthermore, grain boundaries were straight and not irregular, as is typical of dynamic recrystallization via grain boundary migration as occurs in the dislocation creep regime [e.g., *Kamb*, 1972]. Finally, the presence of numerous four-grain junctions, absent in undeformed samples, provide strong evidence for GBS leading to grain switching during superplastic flow [e.g., *Ashby and Verrall*, 1972; *Langdon*, 1991]. Thus our microstructural observations, especially the lack of grain flattening and the presence of numerous four-grain junctions, provide strong evidence that GBS contributes substantially to the deformation in the $n = 1.8$ regime.

At the lowest stresses and the smallest grain sizes the creep rate is characterized by a stress exponent of 2.4 and an activation energy of between 55 and 62 kJ mol^{-1}. This value of the stress exponent is in excellent agreement with those for single crystals of ice oriented for basal slip, as shown in Table 1. The range of values for the activation energy brackets that for volume diffusion in ice, ~60 kJ mol^{-1}, and agrees well with that obtained in creep studies of basal slip in single crystals (see Table 1). In addition to the good agreement between values of n and Q in the $n = 2.4$ regime with those for single crystals deforming by basal slip, the absolute strengths of our polycrystalline samples are in excellent agreement with those for basal slip in single crystals, as shown in Figure 2b [see also *Goldsby and Kohlstedt*, 1997a, Figures 7 and 8]. This regime might be associated with region I observed for superplastic materials [e.g., *Langdon*, 1994]. In the same context, the dislocation creep ($n = 4.0$) regime would correspond to region III reported for superplastic materials.

In Figure 2a the concave down character of the stress-strain rate data at the lowest stresses and smallest grain sizes demonstrates that in polycrystalline ice, superplastic flow and basal slip are serial processes such that the slower process limits the creep rate. Likewise, extrapolation of data from the $n = 1.8$ regime to the temperatures and grain sizes of Figure 2b would indicate faster strain rates at a given stress than are observed. Both GBS and intracrystalline slip on the basal slip system are required for grain-to-grain compatible deformation (i.e., deformation without the formation of voids [e.g., *Paterson*, 1969]) in the $n = 1.8$ and $n = 2.4$ creep regimes. When

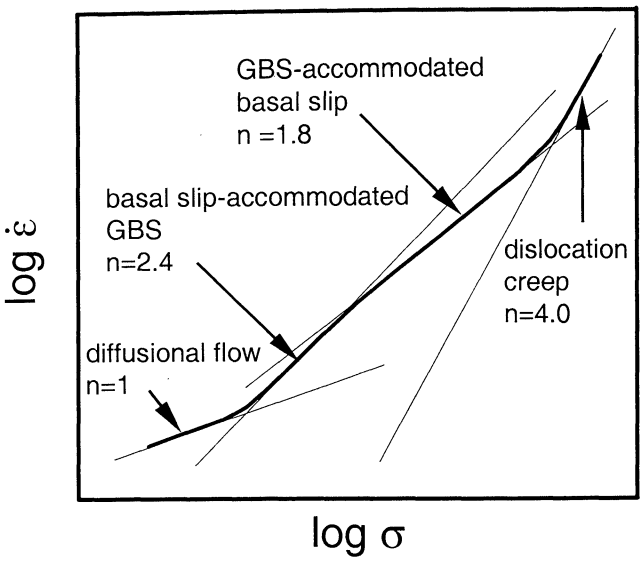

Figure 5. Schematic diagram depicting the relative contributions of each of the four creep mechanisms for ice as a function of stress.

GBS is slower than basal slip, the creep rate of polycrystalline ice is limited by GBS, characterized by n = 1.8. When intracrystalline slip on the basal slip system is slower than GBS, the creep rate is limited by basal slip, characterized by n = 2.4. For the range of conditions explored in our experiments this transition from GBS-limited to basal slip-limited creep occurs at practical strain rates (i.e., above 10^{-8} s^{-1}) only for the finest grained samples. For coarser-grained samples the transition to the basal slip-limited regime occurs at strain rates too slow to allow a significant amount of deformation on a laboratory timescale.

5.2. Summary of Rheology

The flow of ice can be described in terms of four deformation mechanisms: dislocation creep, grain boundary sliding, basal or easy slip, and grain boundary diffusion. As illustrated schematically in Figure 5, four creep regimes characterize the flow of ice over a wide range of stress, strain rate and temperature. At high stresses in the n = 4.0 regime, dislocation creep is the primary deformation mechanism with both basal and nonbasal slip contributing to deformation. With decreasing stress, GBS becomes the rate-controlling mechanism in the superplastic or n = 1.8 regime in which basal slip is accommodated by GBS. At lower stresses, GBS is faster than basal slip such that in the n = 2.4 regime GBS is accommodated by basal slip. Finally, at still lower stresses, grain boundary diffusion creep with n = 1.0 is the dominant deformation process [*Raj and Ashby*, 1971]. This regime has not been observed experimentally for ice even in our low-stress experiments using samples with a grain size as small as 3 μm.

5.3. New Constitutive Equation

As demonstrated by our experimental observations, the flow of ice cannot be adequately described by one flow law with a single set of creep parameters. To date, the flow of glaciers and ice sheets has generally been modeled using the Glen flow law, a power law relation based on the pioneering laboratory experiments of *Glen* [1952, 1955]:

$$\dot{\varepsilon} = B\sigma^n. \qquad (2)$$

In the Glen flow law, n has a value of 3 and B is taken to be constant at a given temperature. Glen's data, shown in Figure 1, lie in the vicinity of the transition from the dislocation creep regime to the superplastic flow regime. Consequently, the Glen law oversimplifies the flow behavior of polycrystalline ice, yielding a single power law with a stress exponent equal to an average value for the slope in the transition region between two creep regimes. As illustrated recently by *Peltier et al.* [2000] and to be demonstrated in detail by D.L. Goldsby and D.L. Kohlstedt (manuscript in preparation, 2001), the superplastic creep regime is very important for the description of the flow of glaciers and ice sheets for which differential stresses are typically <0.1 MPa, values smaller than those explored in Glen's experiments (Figure 1). The Glen law underestimates the creep rate of ice at glaciologically important stresses.

The constitutive equation for the flow of ice is composed of at least 4 individual flow laws of the form of equation (1), one each for dislocation creep, GBS-accommodated basal slip (i.e., "superplastic flow"), basal slip-accommodated GBS, and diffusional flow. On the basis of our experimental observations as illustrated in Figure 5, we propose the following constitutive equation as modified from *Goldsby and Kohlstedt* [1997b]:

$$\dot{\varepsilon} = \dot{\varepsilon}_{diff} + \left(\frac{1}{\dot{\varepsilon}_{basal}} + \frac{1}{\dot{\varepsilon}_{gbs}} \right)^{-1} + \dot{\varepsilon}_{disl}, \qquad (3)$$

where the subscripts refer to diffusional flow (diff), basal or easy slip (basal), grain boundary sliding (gbs), and dislocation creep (disl). Each of the terms on the right-hand side of equation (3) can be described by a flow law of the form given in equation (1). Our experimentally determined flow law parameters for each creep mechanism are listed in Table 5. We have determined flow laws for all of the individual components in equation (3) except diffusional flow. Below, we will estimate the diffusional flow rate using our experimental data as constraints.

To compare our constitutive equation, which includes both dislocation and grain size sensitive flow mechanisms, with

Table 5. Constitutive Equation Parameters

Creep Regime	A, units	n	Q, kJ mol^{-1}
Dislocation creep (T<258 K)	4.0×10^5 MPa$^{-4.0}$ s^{-1}	4.0	60
Dislocation creep (T>258 K)	6.0×10^{28} MPa$^{-4.0}$ s^{-1}	4.0	~18
GBS-accommodated basal slip (T<255 K)	3.9×10^{-3} MPa$^{-1.8}$ m$^{1.4}$ s^{-1}	1.8	49
GBS-accommodated basal slip (T>255 K)	3.0×10^{26} MPa$^{-1.8}$ m$^{1.4}$ s^{-1}	1.8	~192
Basal slip-accommodated GBS	5.5×10^7 MPa$^{-2.4}$ s^{-1}	2.4	60

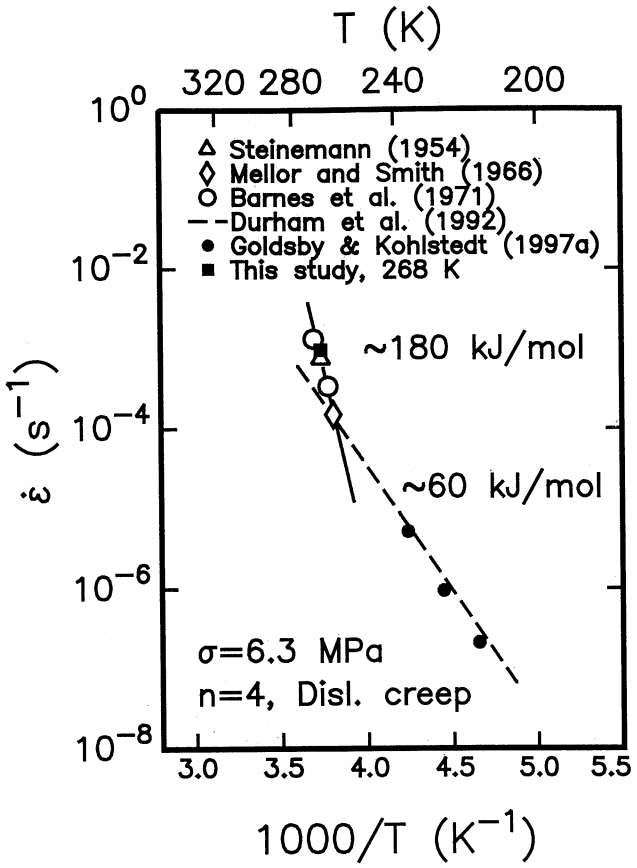

Figure 6. Arrhenius plot containing the data used to estimate the increase in apparent activation energy for dislocation creep above ~258 K. Data are normalized to a stress of 6.3 MPa. The activation energy above 258 K is approximated as 181 kJ mol^{-1}.

previous laboratory data, we extrapolate our constitutive equation to the larger grain sizes and higher temperatures used in most laboratory creep experiments. Three further refinements are first required to take into account the increase in the apparent activation energy for dislocation creep at higher temperatures, the rate of diffusional flow, and the enhancement in the diffusional flow rate due to premelting.

5.4. Enhanced Rate of Dislocation Creep Above 258 K

At $T \geq 258$ K the rate of dislocation creep is faster than predicted by extrapolating the lower temperature results. This softening at higher temperatures is caused by "premelting" at grain boundaries and/or three- and four-grain junctions at temperatures below the freezing point [*Dash et al.*, 1995]. This conclusion is supported by the observation that creep experiments on single crystals of ice reveal no corresponding increase in Q at similar temperatures [*Homer and Glen*, 1978]. This enhancement in dislocation creep rate is difficult to quantify because relatively few data exist for ice deformed in the dislocation creep regime above 258 K. Most studies in Table 2 that yield an increase in Q to >120 kJ mol^{-1} at T >263 K have been conducted in the transition region between dislocation creep and superplastic flow.

We determined the enhancement in the dislocation creep rate caused by premelting by plotting on the Arrhenius plot in Figure 6 published creep data for coarse-grained samples for which the stress exponent at the highest stresses ($\gtrsim$1 MPa) equals ~4 [e.g., *Steinemann*, 1954; *Mellor and Smith*, 1966; *Barnes et al.*, 1971]. Also plotted is a data point from our study at 268 K (see Figure 3b). All of these data were acquired at or normalized to a differential stress of ~6.3 MPa. The dislocation creep flow law calculated using the lower temperature dislocation creep parameters in Table 5 underestimates the dislocation creep rate at, for example, 268 K by a factor of ~5.8. For T >258 K, we approximate the apparent activation energy for dislocation creep as ~180 kJ mol^{-1}.

5.5. Diffusional Flow

Our experiments reveal no evidence for diffusion-accommodated GBS, even for our finest grain sizes of 3-5 μm. The diffusional flow rate is therefore estimated using the diffusion creep equations with our experimental data as constraints. The creep rate due to diffusional flow [*Nabarro*, 1948; *Herring*, 1950; *Coble*, 1963] can be written as

$$\dot{\varepsilon} = \frac{42\,\sigma V_m}{RTd^2}\left(D_v + \frac{\pi\delta}{d}D_b\right), \qquad (4)$$

where V_m is molar volume, D_v is the volume diffusion coefficient, δ is the grain boundary width, and D_b is the grain boundary diffusion coefficient. The diffusion coefficients are each of the form $D = D_o \exp(-Q/RT)$; the symbols $D_{o,v}$ and $D_{o,b}$ along with Q_v and Q_b hereafter designate the preexponential term D_o and the activation energy for volume and grain boundary diffusion, respectively. To estimate the diffusional flow rate, we employed the values listed in Table 6 for the parameters in equation (4).

The volume diffusion coefficients for both hydrogen and oxygen have been determined by a number of researchers (e.g., ^{18}O diffusion [*Kuhn and Thurkauf*, 1958; *Delibaltas et al.*, 1966] and ^{3}H diffusion [*Dengel and Riehl*, 1963; *Itagaki*, 1966; *Ramseier*, 1967a, 1967b]). Values of the diffusion coefficient for the two species are nearly identical. To estimate the rate of volume diffusion creep, we employed the volume diffusion coefficient of *Ramseier* [1967a] for hydrogen diffusion.

Table 6. Diffusion Creep Parameters

Parameter	Value	Comment and/or Reference
Burgers vector, b	4.52×10^{-10} m	*Fletcher* [1970]
Molar volume, V_m	1.97×10^{-5} m^3	*Fletcher* [1970]
Preexponential, volume diffusion, $D_{o,v}$	9.10×10^{-4} m^{2}s^{-1}	*Ramseier* [1967b]
Activation energy, volume diffusion, Q_v	59.4 kJ mol^{-1}	*Ramseier* [1967b]
Grain boundary width, δ	9.04×10^{-10} m	= 2b, after *Frost and Ashby* [1982]
Activation energy, boundary diffusion, Q_b	49 kJ mol^{-1}	*Goldsby and Kohlstedt* [1997a]

A value for the grain boundary diffusion coefficient for ice has not been determined. We therefore estimated D_b for the rate-controlling diffusing species using our experimental data as constraints. It is first assumed that Q_b is equivalent to the activation energy for superplastic flow, 49 kJ mol^{-1}, consistent with results for materials deformed in superplastic region II [*Johnson*, 1970; *Edington et al.*, 1976; *Padmanabhan and Davies*, 1980; *Langdon*, 1994]. A value of Q_b = 49 kJ mol^{-1} is identical to that for grain growth in ice [*Gow*, 1969], a process often rate-limited by boundary diffusion.

The remaining unknown parameter in equation (4), $D_{o,b}$, is constrained using our experimental data. Creep data for samples with grain sizes of 3-5 μm (see Figure 2b) deformed in the basal slip-accommodated GBS (n = 2.4) creep regime show no transition to diffusional flow at the lowest stress, ~2 MPa, and strain rate, ~9 × 10^{-8} s^{-1}, at 208 K. The grain boundary diffusional flow rate at these conditions must therefore be <9 × 10^{-8} s^{-1}. Substitution of these values for stress, strain rate, and temperature with an "average" grain size of ~4 μm, the diffusion creep parameters of Table 5, and our estimated value of Q_b into equations (3) and (4) (and setting D_v = 0) yields an upper bound for $D_{o,b}$ of 8.4×10^{-4} m^2 s^{-1}. This value is nearly identical to the value for $D_{o,v}$ determined by *Ramseier* [1967a]. A similar calculation using data from a 3-5 μm sample deformed at 193 K in the basal slip-accommodated GBS regime [see *Goldsby and Kohlstedt*, 1997a, Figure 5] yields an upper bound for $D_{o,b}$ of 5.8 × 10^{-4} m^2 s^{-1}.

5.6. Enhanced Rate of Diffusional Flow Above 258 K

An enhancement in the rate of Coble creep is expected above 258 K because the presence of a water film along grain boundaries (associated with premelting) would provide a high-diffusivity pathway. An extreme upper bound for the enhancement in Coble creep rate can be estimated by replacing the grain boundary width with the thickness of a grain boundary water film and the grain boundary diffusion coefficient with one near the value for diffusion in water. We estimate a grain boundary film thickness δ_{film} of ~5 nm. The tracer diffusion coefficient in water is 2.5×10^{-9} m^2 s^{-1} at 273 K [*Wang et al.*, 1953]; this value represents an upper bound for the diffusivity in the grain boundary film, given that the assumed grain boundary film is thin enough that its properties would likely not be those of bulk water, but rather those of a structured fluid. We therefore employ a conservative estimate for the film diffusivity D_{film} of 10^{-10} m^2 s^{-1}. Our estimate of the grain boundary diffusion coefficient at 273 K, with $D_{o,b}$ = 6×10^{-4} m^2 s^{-1} and Q_b = 49 kJ mol^{-1}, is ~2.5×10^{-13} m^2 s^{-1}. The enhancement in Coble creep rate caused by the presence of a fluid film is then

$$\frac{\dot{\varepsilon}_{film}}{\dot{\varepsilon}_{Coble}} = \frac{\delta_{film} D_{film}}{\delta_b D_b} . \quad (5)$$

Substituting $\delta_{film} \approx$ 5 nm and $\delta_b \approx$ 1 nm along with values of D_{film} and D_b at 273 K into equation (5) yields a Coble creep rate enhancement of a factor of ~10^3. A larger value of δ_{film} is inconsistent with the modest strain rate enhancements that occur in both the dislocation creep and dislocation-accommodated GBS regimes at T > 258 K, each ~1 order of magnitude at 273 K. The viscosity of a thicker film would be that of bulk water, which would result in a drastic loss of cohesion and strength [e.g., *Pharr and Ashby*, 1983].

In situ microstructural studies of ice near the melting point [*Ketcham and Hobbs*, 1969; *Nye and Mae*, 1972] demonstrate that water in ice at ~273 K also exists in three-grain junctions. The enhancement in Coble creep rate caused by the presence of water in three-grain junctions only (i.e., neglecting premelting along grain boundaries) can be estimated using the model of *Cooper and Kohlstedt* [1984] and *Cooper et al.* [1989]. The presence of fluid in three- and four-grain junctions provides a stress enhancement and a shortened grain boundary diffusion path. The effect on strain rate is a function of the dihedral angle and melt fraction, that is, the shape and size of the three- and four-grain junctions. *Ketcham and Hobbs* [1969] report a dihedral angle of 20°±10° for ice. The Cooper-Kohlstedt model yields an enhancement of only a factor of 2-3 for this dihedral angle for a melt fraction of 0.05, an upper limit based on the in situ measurements at 273 K of *Ketcham and Hobbs* [1969] and *Nye and Mae* [1972]. The effect of water in three-grain junctions on the Coble creep rate of ice is therefore negligible.

5.7. Enhanced Rate of Basal Slip Accommodated GBS Above 258 K

An enhancement in strain rate due to premelting also likely occurs in the basal slip-accommodated GBS (n=2.4) regime. However, as demonstrated in section 5.8, a transition from the n=1.8 to the n=2.4 regime occurs only at very low stresses (~10^{-3}-10^{-2} MPa) even for temperatures near the melting point and small grain sizes (~1 mm). Because basal slip and GBS are serial processes such that the slower process limits the creep rate, an enhancement in creep rate due to basal slip-accommodated GBS (n=2.4) would only serve to broaden the stress range over which GBS-accommodated basal slip (n=1.8) limits the creep rate. Hence the enhancement in creep rate in the n=2.4 regime can safely be neglected in extrapolating our results to larger, glaciologically important grain sizes.

5.8. Comparison of Constitutive Equation With Previous Laboratory Results

Our constitutive equation provides an excellent description of our experimental data; the solid curves in Figure 2a were calculated using the constitutive equation (3) and the appropriate grain sizes. We now compare our data with previous laboratory results by extrapolating our constitutive equation to the larger grain sizes and higher temperatures typical of previous experiments. In Figures 7a-7c a subset of the creep data listed in Tables 1-5 is compared with our constitutive equation for three temperature ranges: 258-264 K, 265-269 K, and 271-273 K.

In Figure 7a the constitutive equation is plotted for a grain size of 1 mm, for temperatures of 264 and 258 K. Predictions of our constitutive equation are in very good to excellent agreement with the data of *Mellor and Smith* [1966] and *Duval and Castelnau* [1995]; both of these data sets exhibit a transition from a stress exponent of 1.8 to a stress exponent of 4.0 at a stress between 0.1 and 1 MPa. However, the constitutive equation underestimates the strain rate for some of the data in the superplastic flow regime. Furthermore, in this regime several of the data sets suggest values of n <1.8. This comparison suggests that at low stresses these data contain significant contributions from transient creep, resulting in a systematically larger underestimation of the steady state strain rate with decreasing stress and thus an underestimation of the

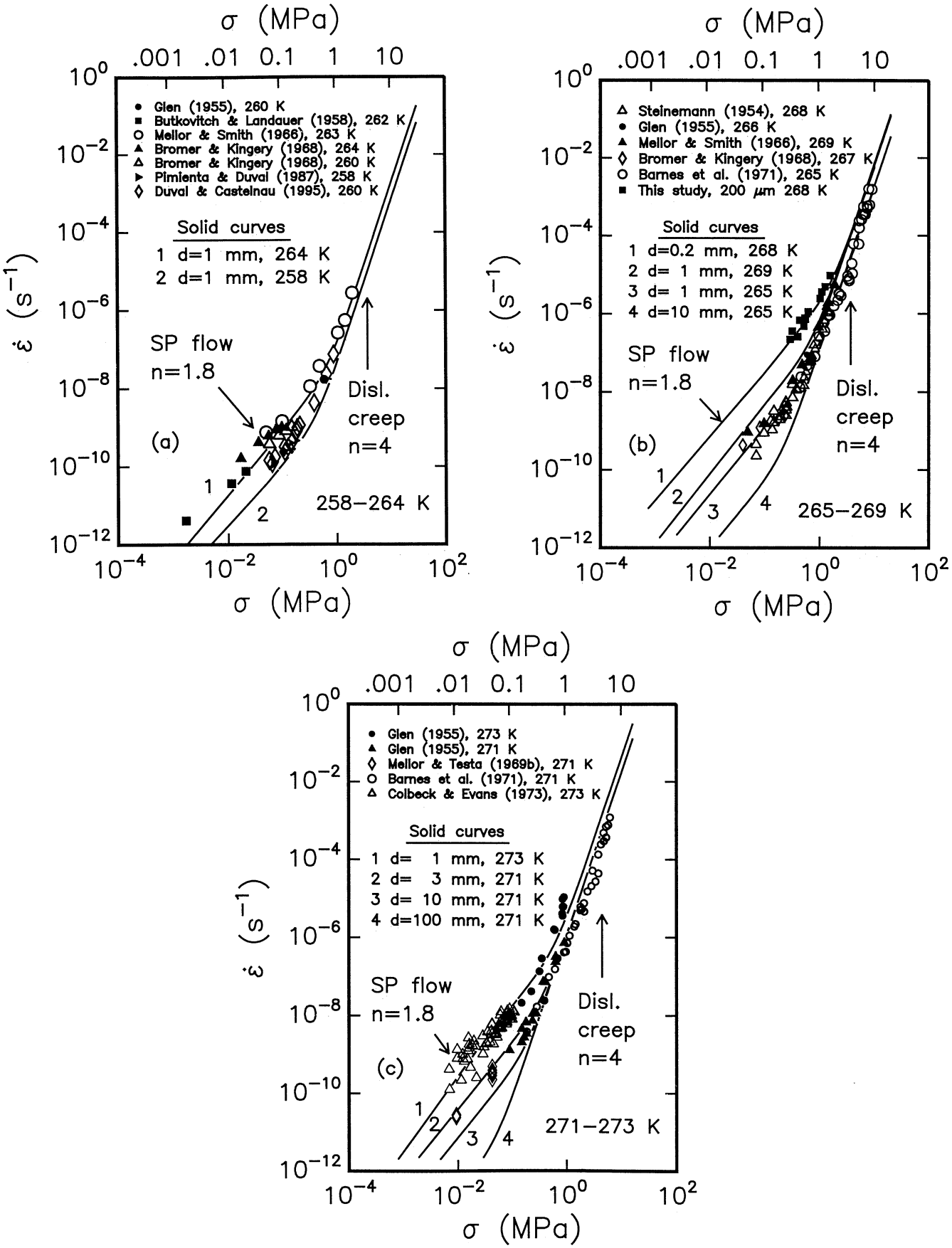

Figure 7. Log-log plots of $\dot{\varepsilon}$ versus σ comparing predictions of the constitutive equation (3) for several different combinations of grain size and temperature with previous creep data acquired in three different temperature ranges. Nearly all of the data are for samples with grain sizes ≥1 mm. (a) T range 258-264 K; (b) T range 265-269 K; (c) T range 271-273 K.

stress exponent. It is expected that this transient creep contribution is also larger at lower temperatures, since at a given stress less strain occurs over a given time period.

In Figure 7b, in addition to comparing our constitutive equation with published creep data, we plot data for our sample with a grain size of ~200 μm that was deformed at 268 K. The constitutive equation is shown for grain sizes of 200 μm and 10 mm at temperatures of 268 and 265 K, respectively. Two additional curves for a grain size of 1 mm at temperatures of 265 and 269 K are included for comparison. Predictions of the constitutive equation in the dislocation creep ($n = 4.0$) regime are in excellent agreement with the data sets of *Steinemann* [1954], *Mellor and Smith* [1969], and *Barnes et al.* [1971], all of which yield a stress exponent of ~4 above a stress of ~0.5 MPa. In the superplastic flow regime ($n = 1.8$) the constitutive equation for a grain size of 1 mm and 265 K is in excellent agreement with the data of *Barnes et al.* [1971] and *Steinemann* [1954]. The data of *Mellor and Smith* [1966] plot at a slightly lower strain rate than predicted by the 1-mm, 269-K curve, possibly because grain growth occurred during these experiments, which were carried out for long times close to the melting point. The experiments of *Mellor and Testa* [1969b], for example, at 271 K were conducted over a period of ~8 months.

Finally, our constitutive equation is compared with previous creep data over the temperature range 271-273 K. As can be seen in Figure 7c, the constitutive equation is in excellent agreement with the data of *Barnes et al.* [1971] and the data of *Glen* [1955] (at 271 K) in the dislocation creep regime. Both data sets yield a stress exponent of 4 above ~0.5 MPa. However, the strain rate in the dislocation creep regime in Glen's experiments near 273 K is a factor of 3 faster than predicted by the constitutive equation. This discrepancy could result from pressure melting at the higher stresses.

In the superplastic flow regime, the data of *Glen* [1955] and *Mellor and Testa* [1969b] at 271 K appear to be in excellent agreement with the predictions of the constitutive equation calculated for a grain size of 3 mm and $T = 271$ K. Grain sizes are not reported by *Glen* [1955]. Mellor and Testa report grain sizes of ~1 mm; however, as discussed above, the experiments were conducted for a total duration of ~8 months. Significant grain growth almost certainly occurred during these experiments; using the grain growth data of *Gow* [1969] (and employing a conservative estimate of the increase in grain growth rate due to premelting at 271 K of 2 orders of magnitude [see *Duval et al.*, 1983]), we estimate that an initial grain size of 1 mm would increase to ~4 mm in 8 months.

Very close to 273 K, the creep data of *Colbeck and Evans* [1973] and *Glen* [1955] in the superplastic flow regime are in good agreement with the constitutive equation calculated for a grain size of 1 mm. Colbeck and Evans report grain sizes of 1-2 mm. Their experiments were conducted on glacier ice in a natural laboratory. That is, the creep experiments were performed in creep apparatus placed in a tunnel excavated in the Blue Glacier in Washington on large blocks of ice cut out of the walls of the tunnel.

On the basis of the very favorable comparison of our constitutive equation with previous laboratory data, we conclude that the transition in creep behavior observed for coarse-grained samples at low stresses represents a transition from dislocation creep with $n = 4.0$ to superplastic flow with $n = 1.8$. A single power law expression is therefore inadequate to describe the rheology of ice over wide ranges of temperature, grain size, and stress; a constitutive equation describing the rheology of ice over a wide range of conditions must contain flow laws for at least four creep mechanisms.

5.9. Implications for Flow in Glaciers, Ice Sheets, and Icy Satellites

Shear stresses τ ($= \sigma/\sqrt{3}$) within glaciers and ice sheets are typically $\lesssim$0.1 MPa; grain sizes are typically 1 mm to several centimeters in size; and temperatures range from ~233 K to 273 K. A transition to the basal slip-accommodated GBS creep regime (that is, the $n = 2.4$ regime) is predicted only at the highest temperatures at stresses $\lesssim$ 0.01 MPa for grain sizes $\lesssim$1 mm, as shown in Figure 7c. Similarly, a transition to diffusional flow is not predicted for grain sizes $\gtrsim$1 mm at temperatures above 233 K over the stress range 0.001-0.1 MPa. Therefore we conclude that superplastic flow is the rate-limiting creep mechanism over most glaciologically significant stresses, grain sizes and temperatures. D.L. Goldsby and D.L. Kohlstedt (manuscript in preparation, 2001) will explore in more detail the implications of the superplastic flow regime for glaciers and ice sheets by comparing our constitutive equation with rheological data from glacier field observations. Superplastic flow is also expected to dominate the rheology of ice in the high overburden, low differential stress environment of icy planetary interiors.

6. Conclusions

1. One-atmosphere creep experiments on fine-grained ice confirm that dislocation creep in ice is characterized by a stress exponent of 4.0 and is independent of grain size.

2. A new creep regime characterized by a stress exponent of 1.8 and a grain size exponent of 1.4 was discovered at low stresses and fine grain sizes. In this superplastic regime, basal slip is accommodated by GBS.

3. At still lower stresses, a third creep regime was identified, characterized by a stress exponent of 2.4. In this grain size insensitive regime, GBS is accommodated by basal slip.

4. On the basis of estimates of diffusion parameters constrained by our experimental observations, we conclude that diffusional flow in ice is unattainable at laboratory strain rates for grain sizes $\gtrsim$3 μm.

5. Our activation energy for dislocation creep of ~60 kJ mol^{-1} is consistent with published values. The activation energies for superplastic flow and basal slip-accommodated GBS creep, based on our results, are 49 and ~60 kJ mol^{-1}, respectively. The activation energies in all three creep regimes increase due to premelting at temperatures above ~258 K.

6. Predictions of our constitutive equation, which is based on the published flow law for dislocation creep of *Durham et al.* [1992] combined with our new flow laws for superplastic flow and basal slip-accommodated GBS, are in excellent agreement with published creep data for coarse-grained ice.

7. Extrapolation of the constitutive equation to larger grain sizes and higher temperatures demonstrates that over a wide range of conditions, including those occurring in glaciers, ice sheets and icy planetary interiors, superplastic flow is the rate-limiting creep mechanism.

Acknowledgments. Support for this research was provided by NASA through grant NAG5-6797. William Durham generously allowed us to use his high-pressure apparatus at Lawrence Livermore National Laboratory and provided numerous stimulating discussions,

valuable insights, and enthusiastic encouragement. Steve Kirby, Laura Stern, and John Pinkston of the U.S. Geological Survey contributed scientific discussions, laboratory facilities, and logistical support. Sriram Viswanathan, Shenghua Mei, Mark Zimmerman, Martha Daines, Yaqin Xu, and Greg Hirth participated in many animated, clarifying discussions throughout the course of this study. Hans Weertman, Terry Langdon, and an anonymous reviewer made critical comments on the manuscript. Shenghua Mei provided invaluable help with the final editing of this paper.

References

Ashby, M.F., and R.A. Verrall, Diffusion-accommodated flow and superplasiticity, *Acta Metall.*, *21*, 149-163, 1973.

Baker, R.W., The influence of ice crystal size on creep, *J. Glaciol.*, *21*, 485-500, 1978a.

Baker, R.W., The influence of ice-crystal size and dispersed-solid inclusions on the creep of polycrystalline ice, PhD. dissertation, 110 pp., Univ. of Minn.-Twin Cities, Minneapolis, 1978b.

Ball, A., and M.M. Hutchison, Superplasticity in the aluminum-zinc eutectoid, *Metal Sci. J.*, *3*, 1-7, 1969.

Barnes, P., D. Tabor, and J.C.F. Walker, The friction and creep of polycrystalline ice, *Proc. R. Soc. London, Ser. A*, *324*, 127-155, 1971.

Bromer, D.J., and W.D. Kingery, Flow of polycrystalline ice at low stresses and small strains, *J. Appl. Phys.*, *39*, 1688-1691, 1968.

Butkovich, T.R., and J.K. Landauer, The flow law for ice, *IAHS Publ.*, *47*, 318-327, 1958.

Butkovich, T.R., and J.K. Landauer, Creep of ice at low stresses, *CRREL Res. Rep.*, *72*, 6 pp., 1960.

Coble, R.L., A model for boundary diffusion controlled creep in polycrystalline materials, *J. Appl. Phys.*, *34*, 1679-1682, 1963.

Colbeck, S.C., and R.J. Evans, A flow law for temperate glacier ice, *J. Glaciol.*, *12*, 71-86, 1973.

Cooper, R.F., and D.L. Kohlstedt, Solution-precipitation enhanced diffusional creep of partially molten olivine-basalt aggregates during hot-pressing, *Tectonophysics*, *107*, 207-233, 1984.

Cooper, R.F., D.L. Kohlstedt, and K. Chyung, Solution-precipitation enhanced creep in solid-liquid aggregates which display a non-zero dihedral angle, *Acta Metall.*, *37*, 1759-1771, 1989.

Dash, J.G., H.Y. Fu, and J.S. Wettlaufer, The premelting of ice and its environmental consequences, *Rep. Prog. Phys.*, *58*, 115-167, 1995.

Davies, G.J., J.W. Edington, C.P. Cutler, and K.A. Padmanabhan, Superplasticity: A review, *J. Mater. Sci.*, *5*, 1-101, 1970.

Delibaltas, P., O. Dengel, D. Helmreich, N. Riehl, and H. Simon, Diffusion of O^{18} in ice single crystals, *Phys. Kondens. Mater.*, *5*, 166-170, 1966.

Dengel, O., and N. Riehl, Diffusion of protons in ice crystals, *Phys. Kondens. Mater.*, *1*, 191-196, 1963.

Durham, W.B., S.H. Kirby, H.C. Heard, L.A. Stern, and C.O. Boro, Water ice phases II, III, and V: Plastic deformation and phase relationships, *J. Geophys. Res.*, *93*, 10,191-10,208, 1988.

Durham, W.B., S.H. Kirby, and L.A. Stern, Effects of dispersed particulates on the rheology of water ice at planetary conditions, *J. Geophys. Res.*, *97*, 20,883-20,897, 1992.

Durham,W. B., L. A. Stern, and S. H. Kirby, Grain size dependent creep of ice I at low temperature; Preliminary results, *Eos Trans. AGU, 75*(44), Fall Meet. Suppl., F635, 1994.

Durham,W. B., S. H. Kirby, and L. A. Stern, Creep of water ices at planetary conditions: A compilation, *J. Geophys. Res.*, *102*, 16,293-16,302, 1997.

Durham,W. B., L. A. Stern, and S. H. Kirby, Rheology of ice I at low stress and elevated confining pressure, *J. Geophys. Res.*, this issue.

Duval, P., and O. Castelnau, Dynamic recrystallization of ice in polar ice sheets, *J. Phys. IV*, *5*, 197-205, 1995.

Duval, P., M.F. Ashby, and I. Anderman, Rate-controlling processes in the creep of polycrystalline ice, *J. Phys. Chem.*, *87*, 4066-4074, 1983.

Edington, J.W., K.N. Melton, and C.P. Cutler, Superplasticity, *Prog. Mater. Sci.*, *21*, 61-170, 1976.

Fletcher, N.H., *The Chemical Physics of Ice,* 271 pp., Cambridge Univ. Press, New York, 1970.

Frost, H.J. and M.F. Ashby, *Deformation Mechanism Maps,* 167 pp., Pergamon, Tarrytown, N.Y., 1982.

Glen, J.W., Experiments on the deformation of ice, *J. Glaciol.*, *2*, 111-114, 1952.

Glen, J.W., The creep of polycrystalline ice, *Proc. R. Soc. London, Ser. A*, *228*, 519-538, 1955.

Gold, L.W., Activation energy for creep of columnar-grained ice, in *Physics and Chemistry of Ice*, edited by E. Whalley, S.J. Jones, and L.W. Gold, pp. 362-364, R. Soc. of Can., Ottawa, Canada, 1973.

Goldsby, D.L., Superplasticity in ice, Ph.D. thesis, Univ. of Minn.-Twin Cities, Minneapolis, 1997.

Goldsby, D.L., and D.L. Kohlstedt, Diffusion creep in ice, *Proc. U.S. Rock Mech. Symp., 35th,* 199-206, 1995a.

Goldsby, D.L., and D.L. Kohlstedt, Grain size sensitive creep of ice, *Eos Trans. AGU, 76*(46), Fall Meet. Suppl., F584, 1995b.

Goldsby, D.L., and D.L. Kohlstedt, Grain boundary sliding in fine-grained Ice I, *Scr. Mater.*, *37*, 1399-1406, 1997a.

Goldsby, D.L., and D.L. Kohlstedt, Flow of ice I by dislocation, grain boundary sliding, and diffusion processes, *Proc. Lunar Planet. Sci. Conf., 28th*, 429-430, 1997b.

Goldsby, D.L., and D.L. Kohlstedt, Dislocation, dislocation-accommodated grain boundary sliding, and diffusion creep of ice I, *Eos Trans. AGU, 78*(46), Fall Meet. Suppl., F723, 1997c.

Goldsby, D.L., D.L. Kohlstedt, and W.B. Durham, Rheology of water and ammonia-water ices, *Proc. Lunar Planet. Sci. Conf., 24th,* 543-544, 1993.

Gow, A.J., On the rates of growth of grains and crystals in south polar firn, *J. Glaciol.*, *8*, 241-252, 1969.

Griggs, D.T., and N.E. Coles, Creep of single crystals of ice, *SIPRE Rep. 11*, 24 pp., Cold Reg. Res. Eng. Lab., N.H., 1954.

Hawkes, I., and M. Mellor, Deformation and fracture of ice under uniaxial stress, *J. Glaciol.*, *11*, 103-131, 1972.

Herring, C., Diffusional viscosity of a polycrystalline solid, *J. Appl. Phys.*, *21*, 437-444, 1950.

Higashi, A., Mechanisms of plastic deformation in ice single crystals, in *Proceedings of the International Conference on Low Temperature Science, 1966*, vol. 1, pp. 277-289, Inst. of Low Temp. Sci., Hokkaido Univ., Sapporo, Japan, 1967.

Homer, D.R., and J.W. Glen, The creep activation energies of ice, *J. Glaciol.*, *21*, 429-444, 1978.

Itagaki, K., Self-diffusion in ice single crystals, *CRREL Res. Rep.*, *178*, 14 pp., 1966.

Jellinek, H.H.G., and R. Brill, Viscoelastic properties of ice, *J. Appl. Phys.*, *27*, 1198-1209, 1956.

Johnson, R.H., Superplasticity, *Metal. Rev.*, *146*, 115-134, 1970.

Jones, S. J., and J.W. Glen, Mechanical properties of single crystals ice at low temperatures, *IAHS Publ.*, *79*, 326-340, 1968.

Jones, S. J., and J.W. Glen, The mechanical properties of single crystals of pure ice, *J. Glaciol.*, *8*, 463-473, 1969.

Kaibyshev, O.A., *Superplasticity of Alloys, Intermetallides and Ceramics*, 317 pp., Springer-Verlag, New York, 1992.

Kamb, B., Experimental recrystallization of ice under stress, in *Flow and Fracture of Rocks, Geophys. Monogr. Ser.*, vol.16, edited by H.C. Heard et al., pp. 211-241, AGU, Washington, D.C., 1972.

Ketcham, W.M., and P.V. Hobbs, An experimental determination of the surface energies of ice, *Philos. Mag.*, *19*, 1161-1173, 1969.

Kirby, S.H., W.B. Durham, M.L. Beeman, H.C. Heard, and M.A. Daley, Inelastic properties of ice Ih at low temperatures and high pressures, *J. Phys.*, *48*, 227-232, 1987.

Kuhn, W., and M. Thuerkauf, Separation of isotopes on freezing of water and the diffusion coefficients of D and O^{18} in ice, *Helv. Chim. Acta*, *41*, 938-971, 1958.

Langdon, T.G., Grain boundary sliding as a deformation mechanism during creep, *Philos. Mag.*, *22*, 689-700, 1970.

Langdon, T.G., The physics of superplastic deformation, *Mater. Sci. Eng. A*, *137*, 1-11, 1991.

Langdon, T.G., A unified approach to grain boundary sliding in creep and superplasticity, *Acta Metall., 42*, 2437-2443, 1994.

Mackwell, S.J., D.L. Kohlstedt, and W.B. Durham, High-resolution creep apparatus, in *The Brittle-Ductile Transition in Rocks: The Heard Volume, Geophys. Monog. Ser.*, vol. 56, edited by A.G.Duba et al., pp. 235-238, AGU, Washington, D.C., 1990.

Mellor, M., Creep tests on Antarctic glacier ice, *Nature*, *184*, 717, 1959.

Mellor, M., and J.H. Smith, Creep of snow and ice, *CRREL Res. Rep.*, *220*, 13 pp., 1966.

Mellor, M., and R. Testa, Effect of temperature on the creep of ice, *J. Glaciol. 8*, 131-145, 1969a.

Mellor, M., and R. Testa, Creep of ice under low stress, *J. Glaciol., 8*, 147-152, 1969b.

Mukherjee, A.K., The rate-controlling mechanism in superplasticity, *Mater. Sci. Eng., 8*, 83-89, 1971.

Nabarro, F.R.N., Deformation of crystals by the motion of single ions, in *Report of a Conference on Strength of Solids (Bristol),* pp. 75-90, Phys. Soc., London, 1948.

Nakaya, U., The deformation of single crystals of ice, *IAHS Publ., 47*, 229-240, 1958.

Nye, J.F., and S. Mae, The effect of non-hydrostatic stress on intergranular water veins and lenses in ice, *J. Glaciol., 11*, 81-101, 1972.

Padmanabhan, K.A., and G.J. Davies, Superplasticity, *Mater. Res. Eng., 2*, 1-312, 1980.

Paterson, M.S., The ductility of rocks, in *Physics of Strength and Plasticity*, edited by A.S. Argon, pp. 377-392, MIT Press, Cambridge, Mass., 1969.

Peltier, W.R., D.L. Goldsby, D.L. Kohlstedt, and L. Tarasov, Ice- age ice-sheet rheology: Constraints from the Last Glacial Maximum form of the Laurentide ice sheet, *Ann. Glaciol., 30*, 163-176, 2000.

Pharr, G.M., and M.F. Ashby, On creep enhanced by a liquid phase, *Acta Metall., 31*, 129-138, 1983.

Pimienta, P., and P. Duval, Rate controlling processes in the creep of polar glacier ice, *J. Phys. Colloq., C1, 3*, 243-248, 1987.

Raj, R., and M. F. Ashby, On grain boundary sliding and diffusional creep, *Metall. Trans., 2*, 1113-1127, 1971.

Ramseier, R.O., Self-diffusion in ice monocrystals, *CRREL Res. Rep., 232*, 40 pp., 1967a.

Ramseier, R.O., Self-diffusion of tritium in natural and synthetic ice monocrystals, *J. Appl. Phys., 38*, 2553-2556, 1967b.

Ramseier, R.O., Growth and mechanical properties of river and lake ice, PhD. thesis, Laval Univ., Quebec, Que., Canada, 1972.

Readey, D.W., and W.D. Kingery, Plastic deformation of single crystal ice, *Acta Metall., 12*, 171-178, 1964.

Ridley, N., C.E. Pearson and his observations of superplasticity, in *Superplasticity: 60 Years After Pearson*, edited by N. Ridley, pp. 1-5, Inst. Mater., London, 1995.

Steinemann, S., Results of preliminary experiments on the plasticity of ice crystals, *J. Glaciol., 2*, 404-413, 1954.

Steinemann, S., Resultats experimentaux sur la dynamique de la lgace et leurs correlations ave le mouvement et la petrographie des glaciers, Symposium of Chamonix, 1958, *IAHS Publ., 47*, 184-198, 1958.

Wakahama, G., On the plastic deformation of single crystal of ice, in *Proceedings of the International Conference on Low Temperature Science, 1966*, vol. 1, pp. 292-311, Inst. Of Low Temp. Sci., Hokkaido Univ., Sapporo, Japan, 1967.

Wang, J.H., C.B. Robinson, and I.S. Edelman, Self-diffusion and structure of liquid water, III, Measurement of the self-diffusion of liquid water with H^2, H^3, and O^{18} as tracers, *J. Am. Chem. Soc., 75*, 466-470, 1953.

Weertman, J., Dislocation climb theory of steady-state creep, *Trans. Am. Soc. Metals, 61*, 681-694, 1968.

Weertman, J., Creep deformation of ice, *Annu. Rev. Earth Planet. Sci., 11*, 215-240, 1983.

D. L. Goldsby, Department of Geological Sciences, Brown University, Providence, RI 02912. (David_Goldsby@brown.edu)

D. L. Kohlstedt, Department of Geology and Geophysics, University of Minnesota-Twin Cities, Pillsbury Hall, Minneapolis, MN 55455. (dlkohl@tc.umn.edu)

(Received March 31, 2000; revised August 22, 2000; accepted August 31, 2000.)